OPEN JOURNAL SISTEMS
ISSN:2237-2202

Available on line at Directory of Open Access Journals

Journal of Hyperspectral Remote Sensing 03 (2015) 086-100

Journal of Hyperspectral Remote Sensing
www.ufpe.br/jhrs

Uncertainties in Unmixing of Multi-phase Hyperspectral Data in Reflective Region: Effects of Texture and Fabric

Keshav D. Singh[ζ] and Ramakrishnan D.

Department of Earth Sciences, Indian Institute of Technology Bombay, Powai, Mumbai-400 076, India

[ζ]**Corresponding Author:** Department of Earth Sciences, Indian Institute of Technology Bombay, Powai, Mumbai-400076, India. Tel.: +91-9699226470 (M)
E-mail address: ksingh86@alumni.uwo.ca (Singh, K. D.)

Received 09 November 2015; received in revised from 15 November 2015: accepted 15 November 2015

Abstract

The Linear Mixing Model (LMM), based on the assumption of single scattering of light is the most preferred approach to unmix (interpret) hyperspectral data due to its simplicity in implementation. However, in most of the natural situations, the reflection process involves multiple scattering and hence, LMM is not very effective. Therefore, nonlinear spectral unmixing model based on Radiative Transfer Equation (RTE) is necessary to understand the influencing factors and effects associated with shadowing or multiple scattering. The reflected spectrum of two juxtaposed materials is the linear sum of the two individual absorption spectra. However, light reflected off an intimate mixture of particles exhibits a spectra that is a nonlinear combination of the two individual spectra. In this work, we have studied the influence of texture (grain size) and fabric (patterns) on reflectance spectra using RTE based nonlinear unmixing model. For this purpose, three types of geological materials namely basalt, anorthosite, and quartzite representing high, moderate and low albedos were used. Multi-phase reflectance spectra of these rocks were acquired in varying combinations of grain size (2-4 mm, 1-2 mm, and <1mm) and patterns. The complexity of fabric was progressively increased from a three-boundary case to intimate mixture. Bi-directional reflectance spectra for different phase angles were collected using a spectroradiometer mounted on a goniometer setup. Subsequently, salient parameters addressing nonlinearity in Hapke model such as phase function, opposition effect, type of scattering for each combination of texture and fabric were estimated from the iteratively modeled spectra. The condition adopted to evaluate the modeling efficacy is the root mean square error (RMSE) between the measured and modeled spectra. When the desired RMSE (<0.01) is achieved, the iteration process is stopped and Hapke parameters corresponding to the best-fit model were retrieved. Analyses of results indicate that grain size, shape, and the fabric cumulatively influence the Hapke parameters such as B_o, b, and c. This clearly indicates that texture and fabric influence the basic physical properties of light scattering namely opposition effect, phase function, and forward/backward scattering property.

Keywords: Bidirectional reflectance, Hyperspectral data, Non-linearity, Hapke's model, Spectral unmixing, Texture, Fabric

1. Introduction

From remote sensing perspective, the problem of mixed pixel classification is a key issue and many solutions are being developed till date to address it (Bosdogianni *et al.* 1996). Spectral unmixing of the image-derived spectra for constituent materials and their abundances is a new solution to classify mixed pixels (Keshava & Mustard 2002). Linear Mixture Models (LMM), a linear addition of several constituent library spectra (signatures) in weighted proportions, is often employed to unmix the mixed pixels. However, LMM has serious limitations mainly as it cannot address the effects of inherent non-linearity in nature due to multiple scattering (Nash & Conel

1974). The multiple scattering effects of reflected light due to factors like size of objects within field of view, source-sensor geometry introduce non-linearity (Keshava & Mustard 2002). It is also found that if the scale of mixing is large, or macroscopic, then the spectral mixing among different materials are linear, while for microscopic or intimate mixtures the spectral mixing are generally nonlinear (Singer & McCord 1979). In the intimate mixture of materials, each component is randomly distributed and consequently, the incident radiation can experience reflections with multiple substances, and the aggregate reflected radiation may no longer uphold the linear proportions of the constituent substances. For this purpose, Non-linear combination of signature spectra were observed and noted by Nash and Conel (1974) and others (Hapke 1981; Shkuratov *et al.* 1999; Fontanilles & Briottet 2011) for accurate identification of constituent members and their abundances. Typically, rock and soils are intimate mixture of mineral components. Due to this, particles are close to each other on a scattering surface and photons reaching the detector are non-linear in nature, hence NLMM is needed to get accurate information about the associated materials (Jacquemoud *et al.* 1992). The NLMM model developed by Hapke *et al.* (Hapke 1981, 1984, 1986, 1993, 2002; Hapke & Well 1984; Hapke *et. al.* 1998) based on Radiative Transfer Equation (RTE) is now being extensively used among the geological and planetary exploration communities (Helfenstein & Veverka 1987; Johnson *et al.* 1992; Pieters 2009; Pieters 2011; Dhingra *et al.* 2011; Yang *et al.* 2011). A horizontal nonlinear mixing model for composite system (e.g. granular mixtures (r_i)) can be written as in eqn. (1),

$$r_i = f(\{m_i\}_i, \{x_i\}_i, \eta; \lambda) \quad (1)$$

Where, m_i is the i-th intimately mixed end-member spectra with an abundance value x_i. η is the associated spectral noise of n wavelength (λ) channels. Using model-based unmixing one can only know the functional formulation of f (Keshava & Mustard 2002).

In the early 1980's, Hapke proposed a two-stream method incorporating multiple scattering and Bidirectional Reflectance Function (BRF) (Hapke 1981; Hapke & Wells 1984). Subsequently, parameters like phase function, macroscopic roughness, extinction coefficient, coherent backscatter, opposition effect, anisotropic scattering, and effects of porosity were considered by Hapke (1993) and others (Liang & Townshend 1996; Shkuratov *et al.* 1999). Despite the distinct practical advantages of Hapke's model, it is still considered as low accurate (Mischenko *et al.* 1999) due to factors such as uncertainness about asymmetry parameters of phase functions, backscattering effects of densely packed reflectors (Mischenko 1994), computational, and experimental difficulties (Quintano *et al.* 2012).

In this study, we have evaluated the combined effects of parameters that are not so far reported namely, texture (grain size and

shape) and fabric (patterns in which granular materials are arranged) on bidirectional reflectance. For this purpose, samples of basalt, anorthosites and quartzite (representing low, medium and high albedo rocks) pulverized into different grain sizes and arranged in seven different patterns were studied. Finally, estimated Hapke's parameters for 21 texture-fabric combinations were analyzed to understand the impact of texture and fabric on the process of light scattering and its effect on reflectance spectra.

2. Theory

2.1 Bidirectional Reflectance Distribution Function

Based on the surface roughness, source, and sensor geometry, a surface can reflect the incoming radiations in different directions with varying intensities. The function that describes this reflectance characteristic for all source-sensor geometry is the bidirectional reflectance distribution function (BRDF). It is the intrinsic property of a surface that describes the angular distribution of radiation reflected by the surface for all angles of existence and for a given illumination geometry (Coburn & Peddle 2006). Mathematically BRDF f_r [sr^{-1}], is the ratio of sensor radiance dL_r [$W.m^{-2}.sr^{-1}.nm^{-1}$] reflected in an outgoing direction (θ_r, ϕ_r) to the hemispherical irradiance dE_i [$W.m^{-2}.nm^{-1}$] from a specific direction (θ_i, ϕ_i). Here, θ_i, ϕ_i is the source and θ_r, ϕ_r is the sensor's zenith and azimuth angles respectively. The mathematical representation for BRDF is given in eqn. (2) below.

$$f_r\left(\theta_i,\psi_i;\theta_r,\psi_r;\lambda\right)=\frac{dL_r\left(\theta_i,\psi_i;\theta_r,\psi_r;\lambda\right)}{dE_i\left(\theta_i,\psi_i,\lambda\right)} \quad (2)$$

2.2 Hapke Model Description

Using the fundamental principles of radiative transfer theory, Hapke (1981) extended the concepts of Nicodemus (1965) to derived an analytical equation for the bidirectional reflectance function (BRF) of a medium composed of granular particles and applied it to planetary surfaces (e.g. moon, mars). These equations consist of several parameters which accounts for single and multiple scattering for an intimate mixture of minerals. This model is based on assumptions such as (i) particle size is very large as compared to the wavelength of light measuring it; (ii) isotropic single and multiple scatterers within the mixture; and (iii) the angle of source and sensor are well defined from the vertical (Hapke 1981). It is considered that the radiance received at the detector is composed of singly scattered radiance I_s and multiple scattered radiance I_m for the given total irradiance **J**. Hence, **I** represents the cumulative effect of single and multiple scattered components (**I**=I_s+I_m**)**. Considering angle of light incidence (i), emergence (e), and azimuth angle (ψ), Hapke (1981, 1984, 1986, 2002) derieved the photometric function for the bidirectional reflectance (R_c) using below mentioned relationship (eqn. 3).

$$R_c(i,e,\psi) = \frac{I}{J} = \frac{w}{4\pi}\frac{\mu_o}{\mu_o+\mu}\{[1+B(g)]P(g,g') + H(\mu_o)H(\mu) - 1\}S(\theta) \quad (3)$$

Here, μ_o, μ are cosines of angle of incidence (i) and angle of emergence (e); g-phase angle; *w*(λ)-wavelength dependent single scattering albedo; B(g)- opposition effect function; P(g) - phase function; and H(μ)- multiple scattering function. The function for macroscopic roughness S (θ) is also referred to as the topographic shadowing function (Hapke 1984). The parameter θ is a mean topographic slope angle that provides a measure of surface macroscopic roughness in a pixel (shape and roughness of particles). If the target spectra are from relatively fresh areas and at terrain with small-scale roughness, then S (θ) initialized arbitrarily at unity (Hapke 1984). Shepard and Campbell (1998) suggested that the smallest faceted scale is the dominant scale for surface shadowing. In case of larger grain sizes, the θ parameter increases depending on the geological properties (Cord *et al.* 2003). It alters the local incidence and emergence angles. The single scattering albedo (*w*) can be calculated from measured reflectance using following eqn. (4),

$$w = \frac{4r_o}{(1+r_o)^2} \quad (4)$$

where, $\mathbf{r_o}$ is the diffuse reflectance. The function of the isotropic multiple scattering H(y) includes angle of incidence, emergence and the single scattering albedo ***w*** (eqn. 5).

$$H(y) = \frac{1+2y}{1+2y\sqrt{1-w}} \quad (5)$$

Where, y is either μ_o or μ. While deriving the solution for radiative transfer equation for an intimate mixture of minerals the effect of decreasing inter-particle spacing has to be taken into consideration. To account for such effects Hapke introduced another function in the reflectance equation which is known as the backscatter function (B(g)). It takes into account the Shadow Hiding Opposition Effect (SHOE) (Hapke *et al.* 1998) as given in eqn. (6),

$$B(g) = \frac{B_o}{1+(1/h)\tan(g/2)} \quad (6)$$

The parameter ***h*** in above equation characterizes compaction of the regolith and its particle size distribution. The angular width parameter ***h*** is constrained between 0 and 1. An empirical parameter B_o defines amplitude of the opposition effect, with values constrained between 0 and 1. If the particles are opaque, scattered light are from the surface and hence, B_o will be equal to1 (Hapke 1986).

Henyey and Greenstein (1941) introduced a phase function in which the deviation of an asymmetry factor, $-1 \le b \le 1$, varies from the backscattering (b<0) through isotropic scattering (b=0) to forward scattering (b>0). The H-G function has a simple expansion in terms of the Legendre polynomials (Pinty *et al.* 1989). In order to generalize the description of fine grains directional reflectance, Jacquemoud *et al.* (1992) have modified phase function (P(g,g')) as given in eqn. (7)

$$P(g,g') = 1 + b\cos(g) + \frac{c(3\cos^2(g)-1)}{2} + b'\cos(g') + \frac{c'(3\cos^2(g')-1)}{2} \quad (7)$$

The function P (g, g') includes these four parameters associated with the material properties and constrained as interval, b[–2, 2], b'[–2, 2], c[–1, 1], and c'[–1, 1] (Yang et al., 2011). Here, the parameters b and c indicate the phase function form and the nature of scattering respectively. Parameter c generally increases with grain size (c>0 corresponds to the backward scattering (g=π) and c<0 to the forward scattering (g=0)) (Jacquemoud *et al.* 1992). cos(g) and cos(g') can be evaluated with values of i, e and ψ using following equations:

$$\cos(g) = \cos(i)\cos(e) + \sin(i)\sin(e)\cos(\psi)$$
$$\cos(g') = \cos(i)\cos(e) - \sin(i)\sin(e)\cos(\psi) \quad (8)$$

2.3 Criteria for Parameters Retrieval

Hapke's parameters address the influencing variables on the measured reflectance spectra (R_m) (Cord *et al.* 2003). In this study, the optimum values of Hapke parameters (p) are retrieved when the Root Mean Square Error (RMSE), (eqn.9) between the measured and modeled reflectance spectra were the least.

$$RMSE = \sqrt{\sum_{k=1}^{n} [R_m(k) - R_c(k, p)]^2} \quad (9)$$

Here, $R_m(k)$ and $R_c(k,p)$ are the measured and calculated bidirectional reflectance over *n* wavelength (λ) channels for the same measurement geometry k = (i, e, ψ) and parameter set p= p(*w*, B_o, h, b, c, b', c'; λ) respectively. Observed reflectance $R_m(k)$ is used to calculate single scattering albedo w using eqn. (4). This calculated w is further used as an input parameter for calculating $R_c(k, \rho)$. Normally, an error (η) up to second decimal is considered as efficient matching.

3. Methodology

3.1 Sample Preparation

To evaluate the effects of texture (grain size), and fabric(patterns) on the bidirectional reflectance, we used three rock samples Basalt (B), Anorthosite (A) and Quartzite (Q) representing the low, moderate and high albedo. These field sampling sites are located around Mamandur Polymetal Deposit, India (northern latitudes 11°52' to 12°01' and eastern longitudes 78°53' to 78°59'). These rocks are subsequently crushed and sieved to three range grain sizes namely, 2mm-4mm, 1mm-2mm, and <1mm. Since shape of the grains influence scattering of light, attempt was also made to investigate the circularity of the grains. For this purpose, grains of above size grades were analyzed for circularity. The circularity index (CI-ratio of cross sectional area of a grain to the area of a circle having the same perimeter as the grain) of the grains are evaluated using a digital photograph and ARC/INFO software (Ramakrishnan *et al.* 2013). Subsequently, these grains are arranged in different test patterns (120° radial, 60° radial, concentric rings, and intimate mixture) with increasing interfaces/boundaries (Fig. 1). For each mixed patterns, the surface abundance of all the three rocks were maintained at 33.33% each. In all, 21 combinations representing three texture classes and seven fabrics were studied.

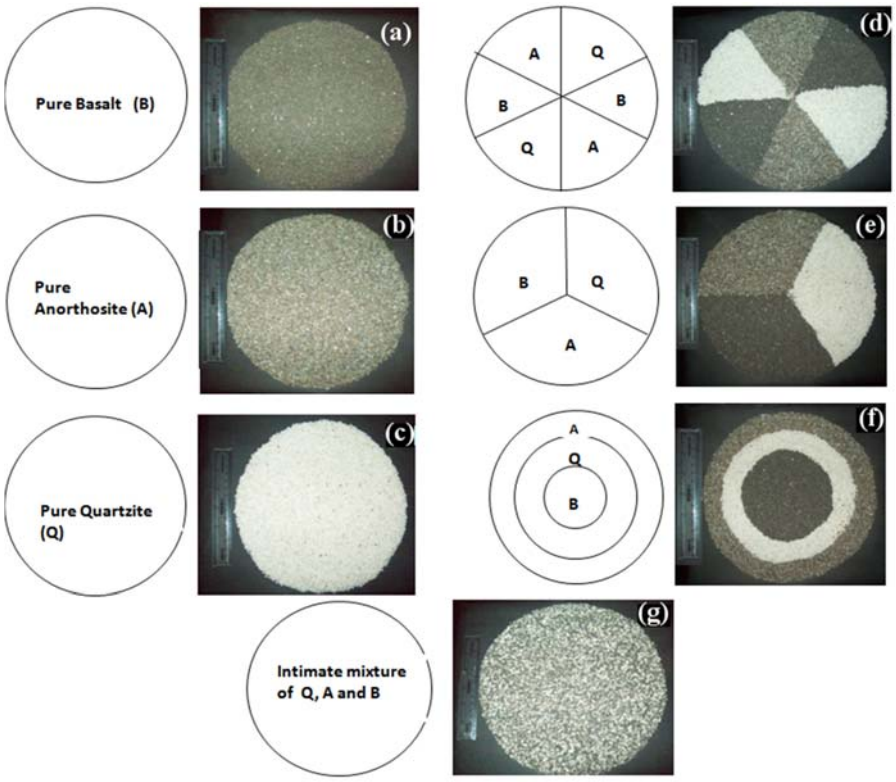

Figure 1: Investigated fabric patterns involving high (quartz), moderate (anorthosite), and low (basalt) albedo rocks for bidirectional reflectance measurement.

3.2 Experimental design and data preprocessing

A goniometer system with adjustable source-sensor geometry was used to measure Bidirectional Reflectance Distribution Function (BRDF) of samples mentioned previously. Samples of adequately larger size (7.85 inches diameter) were used to avoid any adjacency effect within the field of view (FOV). The source lamp was kept at near nadir (5^{o}) position to achieve good illumination. Subsequently, bidirectional reflectance spectra of the samples were collected for an azimuth (ψ) resolution of 30^{o}and zenith (e) resolution of 5^{o}. The Analytical Spectral Devises (ASD) spectroradiometer Fieldspec-3 was calibrated using spectralon reference following the standard spectral acquisition protocol (Salisbury, 1998). The experiments were conducted in a dark room to avoid contamination from stray light. Resultantly, 1134 measurements (3 texture classes' × 7 fabrics × 9 zenith planes × 6 azimuthal planes) were made to understand the effects of texture and fabric on bidirectional reflectance. The spectra collected by above experiments were analyzed for scattering anisotropy and spectral shape changes. Since the minerals in chosen rock samples have characteristic vibration, the reflectance spectra for each combination shows varies depths and different spectral properties (Bharti *et al.* 2012).

3.3 Hapke's parameters Retrieval

As discussed earlier in section 2.2, the Hapke's theoretical equation involves seven parameters namely, four phase function parameters (b; c; b'; c'), two opposition effect function parameters (h; B_o) and albedo $\boldsymbol{w}$ (λ) that address the spectral nonlinearities (Hapke 1993). These global set of nonlinear parameters (p) were obtained for all experimental cases using an algorithm (Algorithm-1) written in Matlab. To minimize the effects of high frequency noises, the input spectra are smoothened using cubic spline smoothening algorithm (Boor 1978). Backscattering function (B(g)) is less constrained than phase function (p(g)). In fact to better describe backscattering effect, smaller phase angle measurements are needed (Hapke, 1996). Hapke's parameters (except $\boldsymbol{w_\lambda}$) are not wavelength-dependent at the first order. Therefore, using these parameters and Hapke's equation, the single scattering albedo spectrum $\boldsymbol{w}$ (λ) is optimized, for the minimum RMSE between measured (R_m) and modeled (R_c) reflectance spectra. Hapke parameters are treated simultaneously without any a priori assumptions just looping their threshold values, thus limiting the risk of meeting local extremes. These obtained Hapke's parameters are use to describe the integral scattering properties and degree of nonlinearity in all experimental set. Finally, the acquired results are interpreted to get nonlinearly corrected sample spectra and its corresponding mineral abundances.

Algorithm- 1: Hapke Parameters Retrieval Steps

1. **Input** raw data: **BRDF** (r_o)
2. **Initialize:** n, i=5, S=1, k=1, 2,…, (9×6)
3. **for** $0 \le \psi \le 150$ **and** $-20 \le e \le 20$ **do**,
4. **Smoothen:** $R_m \rightarrow$ ***csaps*** ($r_o(k)$)
5. **Compute** w, γ=**sqrt**(1-*w*), H (μ_o), H (μ) g and g' (eqn. **4, 5, 8**)
6. **Compute** $\mu_{ie} = \mu_o / (\mu_o + \mu)$ and $I_m = [\{H(\mu_o) H(\mu)\} - 1]$
7. **for** $0.1 \le h \le 1.0$ and $0.1 \le B_o \le 1$ **do**,
8. **Compute** B(g) (eqn. **6**)
9. **for** $-2 \le b \le 2$; $-1 \le c \le 1$; $-2 \le b' \le 2$; $-1 \le c' \le 1$ **do**,
10. **Compute** P(g, g'), I_s, and R_c (cf. eqn. **3, 7**)
11. **Calculate** RMSE value (eqn. **9**)
12. **if** RMSE ~ $\boldsymbol{\eta(O^{-2})}$ **do**,
13. **disp** (i, e, ψ, h, B_o, b, c, b', c'; λ) values and **plot** BRDF {measured (R_m) vs. calculated (R_c)} w.r.t $\boldsymbol{\lambda}$ **else** modify RMSE value and **repeat** algorithm
14. end **if**
15. end **for** loops
16. **set** k→ k+1
17. **end** of computation

4. Results and Discussion

Fig. 2 (a-g) shows the variation in bi-directional reflectance spectra of rocks arranged in accordance to previously mentioned texture and patterns. As expected, the reflectance of quartzite is higher (0.4-0.8) than the anorthosites (0.1-0.5) and basalt (0.05-0.22). Within each category of rocks, fine-grained rocks (< 1mm) have highest reflectance (0.6-0.8 for quartzite, 0.25-0.42 for anorthosites and 0.18-0.22 for basalt) over the medium (1-2mm) and coarse-grained (2-4mm) counterparts (Fig. 3). Conventionally, this observation is attributed to increased scattering efficiency by fine-grained particles (scatterers) and the crystalline composition of the grain is also influences the reflectance. However, the streak-colour of the powder of the rock- can also influence the overall albedo (Bharti *et al.* 2012). For example, an anorthosite fragment, which is grey in colour, becomes whitish when powdered and result in increase of albedo. This property could be attributed to several fold increase (200%) in reflectance values of low albedo rocks like basalt when powdered. To understand the cumulative effect of texture and fabric on the spectral shape, plots between grain size and reflectance were made at wavelengths 700 nm and 1300nm (Figs 4a and b). These two wavelengths correspond to the characteristic absorption features of basalt (due to pyroxene at 700nm) and anorthosites (due to plagioclase at 1300nm) respectively. Since quartzite does not have spectral absorption in these regions, the changes in albedo of resultant mixture can be interpreted as the cumulative effect of texture and fabric on albedo. It is interesting to note that only intimate mixture exhibits the theoretically expected a near linear decrease in albedo (black solid line in Figs 3a and b). In case of radial patterns disposed at 60 and 120 degrees (solid grey line and dotted black line), the albedo corresponding to 2-4mm fractions were higher than 1-2 mm fractions and in case of circular pattern, the trend is exactly reverse.

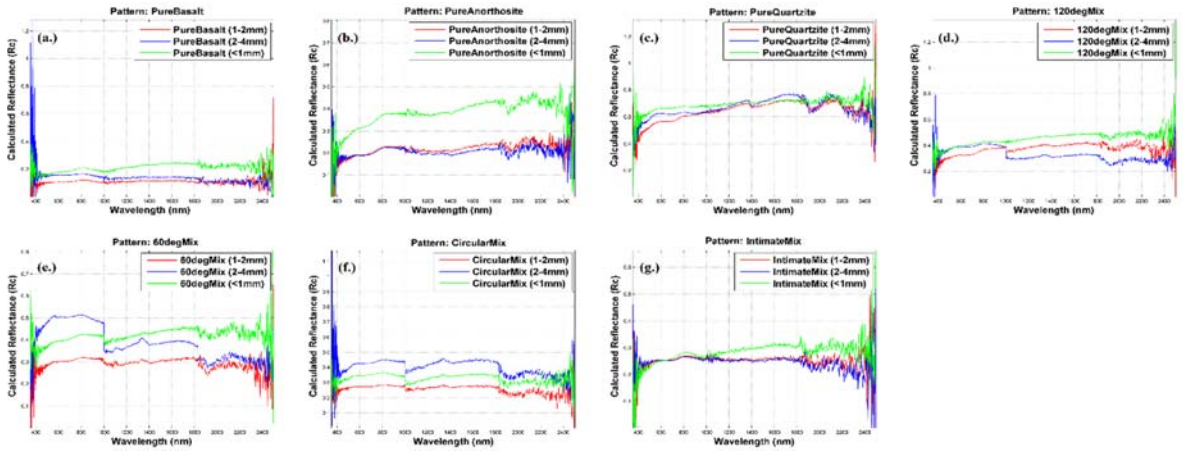

Figure 2: Variations in spectral reflection due to cumulative effect of texture and fabric.

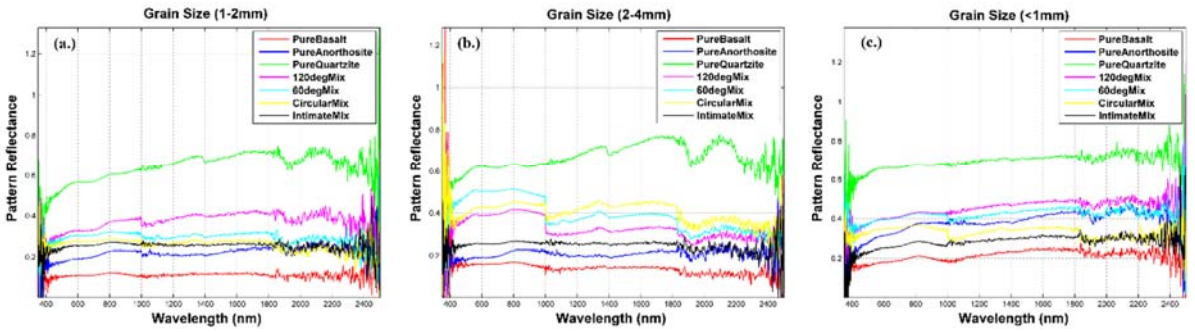

Figure 3: Effect of grains size variations on the reflectance spectra.

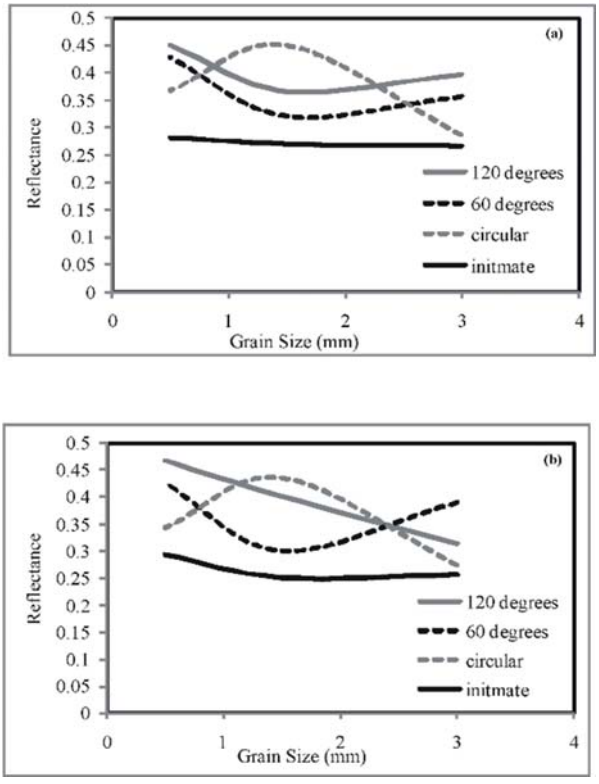

Figure 4: Plot showing reflectance changes at 700nm (a) and 1300 nm (b) in response to changes in texture and fabric.

Since the shape of the scatters also influences scattering, we investigated the shape of grains constituting all the three-grain size ranges. The grain size fragments <1mm are nearly circular with an average Circularity Index (CI) closer to 1.00. Whereas, average CI of 1-2mm fragments are 1.3 and coarser (2-4mm) fragments are 1.5. Since the coarse grains deviate significantly from the spheres, the multiple scattering of light are high, and deviate from the theoretical grain size-scattering relationship. This increased multiple scattering is attributed to slight increase in reflectance values of 2-4mm grains than that of 1-2mm grains in case of alternately disposed high and low albedo rocks. When high albedo

material (quartz) is sandwiched between low albedo materials in concentric circular pattern (Fig. 1f), a relatively low resultant albedo is observed. This phenomenon is again attributed to multiple scattering effects by low albedo basalt and anorthosites having longer, circular boundary with quartz. In this case, the multiple scattering by low albedo materials subdue the effects of high albedo quartz.

To understand and account for the variability introduced by the fabric, shape, and texture, attempt is herein also made to model the reflectance spectra using Hapke equation. The coefficients addressing the non-linear aspects of the light scattering (h, B_o, b, c, b', c') were iteratively retrieved for each one of the above cases (Fig. 5, Table 1). It is evident from above figure and table that for the high albedo material, the model parameters slightly change with the grain size variations. Whereas, for the medium and low albedo rocks, parameters namely B_o and b change considerably when the grain size is changed. In case of samples with variations in fabric and grain size, parameters B_o, b, and c varies. This implies that the variations in fabric and texture cumulatively influence opposition effect, phase function and forward/backward scattering property. In this study, b and c were observed to be the main parameters addressing the fabric and texture related scattering phase function. For lower RMSE value was within 0.03, the estimation values of b, b' met the estimation value of c, c' parameters. Further, from analysis of RMSE vis-à-vis Hapke parameter variability (Table-1, Fig. 5) it is evident that c and c' are more stable than that of b and b' for a range of RMSE. This variability is appreciable when RMSE is greater than 0.03. Generally, when the RMSE value was smaller than 0.03, the relationship among the parameters followed the order: b' <b <c' <c. The variation in parameter b and c reveals that the large grains and high albedo materials result in backward scattering and that small grains and dark materials lead to forward scattering (Cord *et al.* 2003). This clearly indicates that for a given abundance, depending on the distribution of high and low albedo (*w*) materials the base line of the reflectance spectra is shifted (Clark 1999).To evaluate overall efficiency of modeling and retrieval of the Hapke parameters, scatter plots were made between measured (R_m) and modelled (R_c) reflectance spectra (Figs 6a-d). It is evident from the result that the best-fit regression line is linear and highly correlated (R^2 -0.99) for the chosen texture-fabric combinations and source-sensor geometry. This clearly shows that the Modeled Hapke's non-linear parameters are mathematically and physically meaningful and account for the variations in light scattering due to texture, shape and fabric.

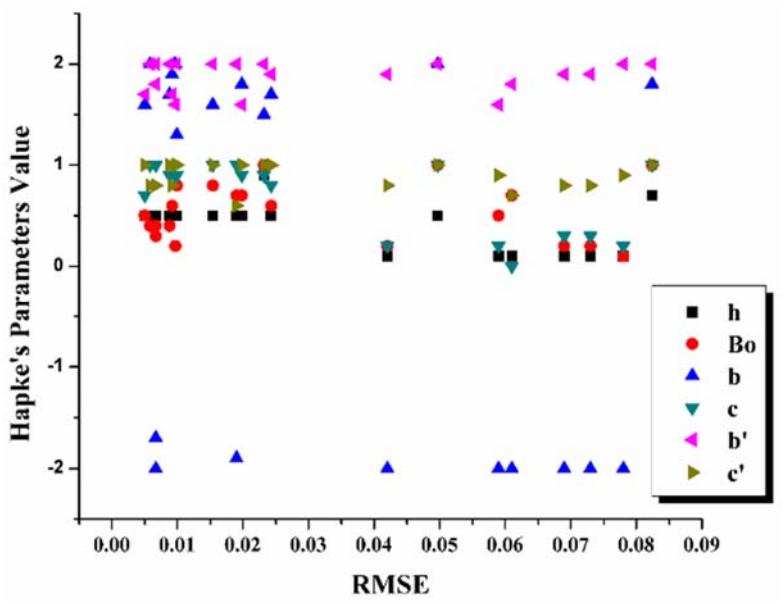

Figure 5: Plots depicting the relationship between retrieved Hapke parameters and associated least possible RMSE.

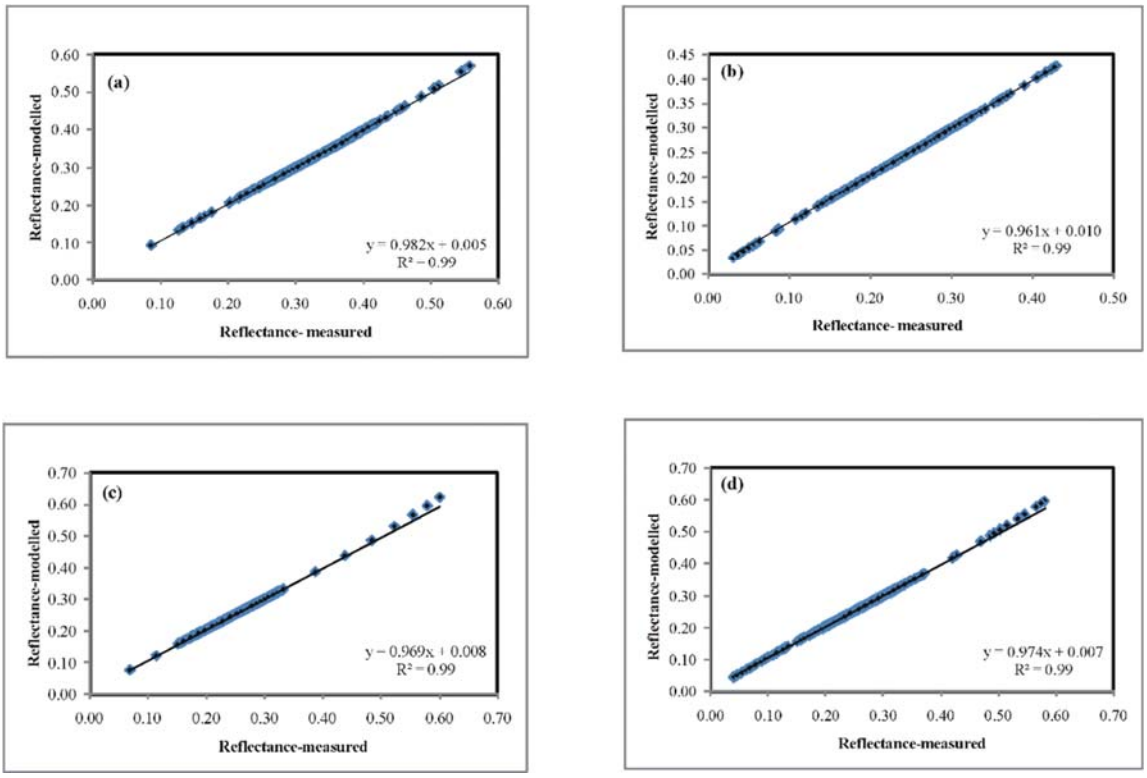

Figure 6: Plot representing the variation of pattern reflectance values with three grain sizes for all patterns at 800nm wavelength.

Table 1: Retrieved Hapke's parameters for different combinations of texture and fabric.

Hapke's Parameters Sample Pattern (Grain size)	i (deg.)	e (deg.)	ψ (deg.)	h	B_o	b	c	b'	c'	RMSE
PureBasalt (2–4mm)	5	-5	0	0.5	0.2	2.0	0.9	1.6	1.0	0.0097
PureBasalt (1–2mm)	5	20	0	0.1	0.2	-2.0	0.2	1.9	0.8	0.0420
PureBasalt (<1mm)	5	0	0	0.5	0.4	-1.7	1.0	1.8	0.8	0.0067
PureAnorthosite (2–4mm)	5	0	0	0.1	0.7	-2.0	0.0	1.8	0.7	0.0610
PureAnorthosite (1–2mm)	5	15	0	0.5	0.3	-2.0	1.0	2.0	0.8	0.0067
PureAnorthosite (<1mm)	5	5	0	0.5	0.7	1.8	0.9	1.6	1.0	0.0198
PureQuartzite (2–4mm)	5	20	0	0.5	1.0	2.0	1.0	2.0	1.0	0.0497
PureQuartzite (1–2mm)	5	20	0	0.7	1.0	1.8	1.0	2.0	1.0	0.0824
PureQuartzite (<1mm)	5	-15	30	0.9	1.0	1.5	0.9	2.0	1.0	0.0232
CircularMix (2–4mm)	5	0	0	0.5	0.7	-1.9	1.0	2.0	0.6	0.0190
CircularMix (1–2mm)	5	20	0	0.1	0.1	-2.0	0.2	2.0	0.9	0.0780
CircularMix (<1mm)	5	0	0	0.5	0.6	1.9	1.0	1.7	0.8	0.0092
120°degMix (2–4mm)	5	0	0	0.1	0.5	-2.0	0.2	1.6	0.9	0.0590
120°degMix (1–2mm)	5	20	0	0.5	0.4	1.7	0.9	2.0	1.0	0.0088
120°degMix (<1mm)	5	-5	0	0.5	0.8	1.6	1.0	2.0	1.0	0.0154
60°degMix (2–4mm)	5	20	0	0.5	0.6	1.7	0.8	1.9	1.0	0.0243
60°degMix (1–2mm)	5	20	0	0.1	0.2	-2.0	0.3	1.9	0.8	0.0690
60°degMix (<1mm)	5	-10	0	0.5	0.8	1.3	0.9	2.0	1.0	0.0099
IntimateMix (2–4mm)	5	5	0	0.5	0.5	1.6	0.7	1.7	1.0	0.0050
IntimateMix (1–2mm)	5	20	0	0.5	0.4	2.0	1.0	2.0	0.8	0.0058
IntimateMix (<1mm)	5	0	0	0.1	0.2	-2.0	0.3	1.9	0.8	0.0730

5. Conclusions

Following are the major outcomes of this study:

1. The size and shape of the mineral grains (texture) and the way they are arranged significantly influence the overall albedo and reflectance spectra of the surface investigated.
2. Influence of texture and fabric on light scattering can be efficiently modeled using Hapke equation and they are observed to influence opposition effect, phase function, and forward/backward scattering properties.
3. Very high correlation between the measured and modeled spectra ($R^2 = 0.99$) indicates that the results are statistically correct and physically meaningful.

6. Acknowledgments

Authors are thankful to the editor JHRS for publication of this work. This work is jointly supported by Department of Science & Technology (DST), Government of India and Indian Institute of Technology Bombay, Mumbai, India.

References

Bharti, R., Ramakrishnan, D., Singh, K.D. & Mullassery, N., 2012. Relevance of mineral texture on bidirectional reflectance and emission spectroscopy: Implications for geological remote sensing, i*n Proceedings of IGARSS,* pp.3046–3049.

Boor, C.D., 1978. *A Practical Guide to Splines*. Springer-Verlag GmbH, Berlin, Germany.

Bosdogianni, P., Petrou, M., & Kittler, J., 1996. Mixed pixel classification in Remote sensing. *International Archives of Photogrammetry and Remote Sensing*, XXXI, Part B7, Vienna.

Clark, R. & Roush, T., 1984. Reflectance spectroscopy: quantitative analysis techniques for remote sensing applications. *Journal Geophysical Research*, 89, 6329–6340.

Clark, R.N., 1999. Spectroscopy of rocks and minerals, and principles of spectroscopy. *Manual of Remote Sensing*, New York, USGS, 3, 3–58.

Coburn, C.A. & Peddle, D.R., 2006. A low-cost field and laboratory goniometer system for estimating hyperspectral bidirectional reflectance. *Canadian Journal of Remote Sensing*, 32(3), 244–253.

Cord, A.M., Pinet, P.C., Daydou, Y. & Chevrel, S.D., 2003. Planetary regolith surface analogs: optimized determination of Hapke parameters using multi-angular spectro-imaging laboratory data. *Icarus*, 165, 414–427.

Dhingra, D., Mustard, J.F., Wiseman, S., Pariente, Pieters, M.C.M. & Isaacson, P.J., 2011. Non-linear spectral unmixing using Hapke's modeling: application to remotely acquired M3 spectra of spinel bearing lithologies on the moon, in *Lunar and Planetary Science Conference*, The Woodlands, Texas, USA, XLII, 2388pp.

Fontanilles, G. & Briottet, X., 2011. A nonlinear unmixing method in the infrared domain. *Applied Optics*, 50, 3666–3677.

Hapke, B. & Wells, E., 1984. Bidirectional reflectance spectroscopy: 2. Experiments and observations. *Journal of Geophysical Research*, 86, 3055–3060.

Hapke, B., 1981. Bidirectional reflectance spectroscopy: 1. Theory. *Journal of Geophysical Research*, 86, 3039–3054.

Hapke, B., 1984. Bidirectional reflectance spectroscopy: 3. Correction for macroscopic roughness. *Icarus*, 59(1), 41–59.

Hapke, B., 1986. Bidirectional reflectance spectroscopy: 4. The extinction coefficient and the opposition effect. *Icarus*, 67, 264–280.

Hapke, B., 1993. Theory of reflectance and Emittance Spectroscopy. *Cambridge Univ. Press*, New York.

Hapke, B., 2002. Bidirectional reflectance spectroscopy: 5. Thec oherent backscatter opposition effect and anisotropic scattering. *Icarus*, 157, 523–534.

Hapke, B., Nelson, R. & Smythe, W., 1998. The opposition effect of the moon: coherent backscatter and shadow hiding. *Icarus*, 133, 89–97.

Helfenstein, P. & Veverka, J., 1987. Photometric properties of lunar terrains derived from Hapke's equation. *Icarus*, 72, 342–357.

Henyey, L.G. & Greenstein, J.L., 1941. Diffuse radiation in the Galaxy. *Astrophysical Journal*, 93, 70–83.

Hiroi, T. & Pieters, C.M., 1994. Estimation of grain sizes and mixing ratios of fine powder mixtures of common geologic minerals. *Journal of Geophysical Research*, 99 (E5), 10867–10879.

Jacquemoud, S., Baret, F. & Hanocq, J.F., 1992. Modeling spectral and bidirectional soil reflectance. *Remote sensing of Environment*, 41, 123–132.

Johnson, P.E., 1983. A semi empirical method for analysis of the reflectance spectra of binary mineral mixtures. *Journal of Geophysical Research*, 88 (B4), 3557–3561.

Johnson, P.E., Smith, M.O. & Adams, J.B., 1992. Single algorithms for remote determination of mineral abundances and particle size from reflectance spectra. *Journal of Geophysical Research*, 97 (E2), 2649–2657.

Keshava, N. & Mustard, J.F., 2002. Spectral unmixing. *IEEE Signal Processing Magazine*, 19(1), 44pp.

Keshava, N., 2003. A Survey of Spectral Unmixing. *Lincoln Laboratory Journal*, 14(1), 55–78.

Liang, S. & Townshend, J.R.G. 1996. A modified Hapke model for soil bidirectional reflectance. *Remote Sensing of Environment*, 55, 110.

Mishchenko, M.I., 1994. Asymmetry parameters of the phase function for densely packed scattering grains. *J. Quant. Spectrosc. Radiat. Transfer*, 52(1), 95–110.

Mishchenko, M.I., Dlugach, J.M., Yanovitskij, E.G., & Zakharova, N.T., 1999. Bidirectional reflectance of flat, optically thick particulate layers: an efficient radiative transfer solution and applications to snow and soil surfaces. *J. Quant. Spectrosc. Radiat. Transfer*, 63, 409–432.

Mustard, J.F., Li, L. & He, G. 1998. Nonlinear spectral mixture modeling of lunar multispectral data: Implications for lateral transport. *Journal of Geophyical Research-Planets*, 103(E13), 19419–19425.

Nash, D.B., Conel, J.E., 1974. Spectral reflectance systematics for mixtures of powdered hypersthene, labradorite, and ilmenite. *Journal of Geophysical Research*, 79(11), 1615–1621.

Nicodemus, F. E., 1965. Directional Reflectance and Emissivity of an Opaque Surface. *Appl. Optics*, 4(7), 767-773.

Pieters, C.M., Besse, S., Boardman, J., Buratti, B., Cheek, L., Clark, R.N., Combe, J.P., Dhingra, D., Goswami, J.N., Green, R.O., Head-III, J.W., Isaacson, P., Klima, R., Kramer, G., Lundeen, S., Malaret, E., McCord, T., Mustard, J., Nettles, J., Petro, N., Runyon, C., Staid,

M., Sunshine, J., Taylor, L.A., Thaisen, K., Tompkins, S. & Whitten, J., 2011. Mg-spinel lithology: A new rock type on the lunar farside. *Journal of Geophysical Research*, 116 E00G08.

Pieters, C.M., Boardman, J., Buratti, B., Chatterjee, A., Clark, R., Glavich, T., Green, R., Head-III, J., Isaacson, P., Malaret, E., McCord, T., Mustard, J., Petro, N., Runyon, C., Staid, M., Sunshine, J., Taylor, L., Tompkins, S., Varanasi, P. & White, M., 2009. The Moon Mineralogy Mapper (M3) on Chandrayaan-1. *Current Science*, 96(4).

Pinty, B., Verstraete, M.M. & Dickinson, R.E., 1989. A Physical Model for Predicting Bidirectional Reflectances over Bare Soil. *Remote Sensing of Environment*, 27, 273–288.

Quintano, C., Fernndez-Manso, A., Shimabukuro, Y.E. & Pereira, G., 2012. Spectral unmixing. *International Journal of Remote Sensing*, 33 (17), 5307–5340.

Salisbury, J.W., 1998. Spectral measurements field guide, unpublished report. *U.S. Defense Technology Information Center Report*, ADA362372, 82pp.

Shepard, M.K. & Campbell, B.A., 1998. Shadows on a planetary surface and implications for photometric roughness. *Icarus*, 134, 279–291.

Shkuratov, Y., Starukhina, L., Hoffmann, H. & Arnold, G., 1999. A model of spectral albedo of particulate surfaces: implications for optical properties of the moon. *Icarus*, 137, 235–246.

Singer, R.B. & McCord, T.B., 1979. Mars: Large scale mixing of bright and dark surface materials and implications for analysis of spectral reflectance, in *Lunar and Planetary Science Conference*, 10th, Houston, Texas, USA, 2, 1835–1848.

Yang, G.J., Zhao, C.J., Huang, W.J. & Wang, J.H., 2011. Extension of the Hapke bidirectional reflectance model to retrieve soil water content. *Hydrology and Earth System Sciences*, 15, 2317–2326.